

Vibrational Circular Dichroism Measurements of Ligand Vibrations in Haem and Non-haem Metalloenzymes

Richard W. Borrett, Gregory D. Smith† and Sanford A. Asher

Department of Chemistry, University of Pittsburgh, Pittsburgh, PA 15260, USA

Doug Barrick

Institute of Molecular Biology, University of Oregon, Eugene, OR 97403, USA

Donald M. Kurtz Jr.

Department of Chemistry and Center for Metalloenzyme Studies, University of Georgia, Athens, GA 30602, USA

We have measured the vibrational circular dichroism (VCD) spectra of the stretching vibrations of azide and cyanide ligated to the Fe^{3+} atoms of haemoglobin (Hb) and myoglobin (Mb). The antisymmetric azide-stretch of the low-spin haems have an anomalously large g -value of *ca.* -1×10^{-3} . In contrast, CN^- has a g -value of *ca.* $+2.4 \times 10^{-3}$. We also show, for the first time, that a significant VCD occurs for the azide ligand antisymmetric stretches of non-haem proteins; we measure a g -value of *ca.* -1×10^{-4} for azide bound to haemerythrin. We have examined the mechanism of the VCD phenomenon by: (1) reconstituting Mb with haems substituted such that they insert differently in the haem pocket; (2) replacing the Fe^{3+} with Mn^{3+} ; (3) examining proteins where replacements occur for E-7 His and E-11 Val distal amino acids close to the haem and (4) examining an Mb mutant where the proximal F-8 His is replaced by Gly, and where an imidazole ligand inserts into the resulting crevice and binds to the haem in a way similar to that of the proximal histidine in the native protein. The VCD anisotropy appears insensitive to the haem substituent replacements used in this study. Exchange of the E-7 distal His or the E-11 Val has a dramatic effect on the g -value. Exchange of the F-8 proximal His reverses the sign of the g -value for the azide complex, but not for the cyanide complex. The work to date indicates that VCD has the potential to become a sensitive technique for examining the structure of metalloenzymes. Work is needed to determine the mechanism giving rise to the large g -values and to correlate the VCD spectrum with the metalloenzyme structure at the active site.

VCD spectroscopy measures the difference in the vibrational transition absorption between left and right circularly polarized light.^{1–6} The VCD phenomenon is due to the chiral constraints on molecular bonding and electronic structure which restrict charge motion induced by the molecular vibration. The chirality of a system is determined either directly by the chirality of its molecular covalent bonding or indirectly by a chiral environment which induces chirality.

The sensitivity of VCD to both molecular structure and environment gives the technique the potential for being uniquely informative for studies of chiral molecular

† Howard Hughes Undergraduate Fellow. Present Address: Centre College, Danville, KY 40422, USA.

systems. The technique could be of unique importance for studying biological molecules because they are always chiral.⁷ For example, proteins are composed of individually connected chiral amino acids. The protein conformation is determined by how it folds; the protein folds into a tertiary structure that is enzymatically active and which has macromolecular chirality. This chiral superstructure is often superimposed on enzyme prosthetic groups, which are chiral either owing to asymmetric substitution or because of induced chirality from the surrounding chiral protein environment.

In this study we explore the use of VCD for examining the ligand-binding geometry and structure of both haem and non-haem metalloenzymes. We reconfirm Marcott *et al.*'s⁸ observation 17 years ago of an anomalously strong VCD for azide ligated to the iron of the haem protein, haemoglobin (Hb). We extend the recent results of Borrett and co-workers^{9,10} by examining Mb reconstituted with haem with altered peripheral substituents, and by a haem where the Fe³⁺ atom is replaced with Mn³⁺ and by a mutant Mb where the F-8 proximal His is replaced by a free imidazole ligand. The purpose of these studies is to determine the factors leading to the large Mb azide ligand anisotropy ($g \approx 10^{-3}$) for the azide antisymmetric stretch.

We also verify Teraoka *et al.*'s observation¹¹ of an even larger VCD anisotropy ($g = +2.4 \times 10^{-3}$) for the CN⁻ complex of Mb. As detailed below we find that the large VCD anisotropy depends upon both the fifth and the sixth axial-ligand geometries and there is little dependence on the haem peripheral substituents or the detailed haem-binding geometry within the globin haem-binding cleft.

We also show that a significant VCD anisotropy for metal-bound ligand vibrations does not require the large aromatic haem ring. We observe a g -value of *ca.* 10^{-4} for azide bound to the non-haem iron of the metalloenzyme haemerythrin.¹²

Our results demonstrate that VCD is an extremely sensitive monitor of haem ligand binding. The sensitivity permits us to monitor subtle changes in the orientation of the ligands in the haem pocket. Utilization of this technique as a structural probe requires, however, an improved understanding of the mechanism which gives rise to the large VCD anisotropy.

Experimental

ApoMb was prepared at 4 °C by dissolving lyophilized horse Mb (Sigma Chemical Company) in potassium phosphate buffer (pH 7, 0.1 mol dm⁻³) to a concentration of 2 mmol dm⁻³. The Mb solution was acidified with hydrochloric acid (1 mol dm⁻³) to pH 2 and the haem was extracted four to five times with equal volumes of methyl ethyl ketone following the method of Teale.¹³ After extraction, the aqueous phase was dialysed against sodium hydrogen carbonate buffer (0.5 mmol dm⁻³), and then dialysed against pure water.

Removal of the haem was confirmed by the disappearance of the haem Soret band absorbance relative to the 280 nm protein band absorbance (>99% haem removal). ApoMb concentrations were determined from the known molar absorptivities.¹³ ApoMb was stable for up to a week if maintained at 4 °C.

The apoMb was reconstituted with iron(III) protoporphyrin IX, iron(III) deuteriohaem and manganese(III) protoporphyrin IX by the dropwise addition of concentrated solutions of the iron chloride salts of these porphyrins (Porphyrin Products) dissolved in sodium hydroxide (0.1 mol dm⁻³). A slight excess of porphyrin was added to the stirred apoMb solutions. The reconstituted Mb were then dialysed overnight *versus* phosphate buffer (0.1 mol dm⁻³, pH 7) and the protein was purified using a Sephadex G-50 gel filtration column (Sigma Chemical Company). All preparations were carried out in a cold room maintained at 4 °C. Molar absorptivities and haem-to-protein peak ratios for deuterioMb, Mn(proto IX)Mb, and the azide bound forms agreed with those in the literature.^{14,15}

Iron(III) etioporphyrin Mb (ETPMb) was prepared by dissolving an excess of the chloride salt of iron(III) etioporphyrin I (Porphyrin Products) in acetone and 5% pyridine. A syringe pump ($6 \text{ cm}^3 \text{ h}^{-1}$) was used to add the ETP to a stirred apoMb solution. Iron(III) protoporphyrin IX dimethylester (DME, Porphyrin Products) was incorporated into apoMb by the dropwise addition of a concentrated solution of the chloride salt dissolved in a solution of 1% pyridine in methanol, into a stirred apoMb solution. Molar absorptivities and haem-to-protein peak ratios for these compounds agreed with previous reports.^{15,16} Azide and CN ligands were added to these solutions to appropriate concentrations. We were unsuccessful in our attempts to reconstitute Iron(III) octaethyl porphyrin into apoMb; we could not get a significant concentration to bind within the haem pocket. The mutant Mb samples and the haemerythrin were prepared as described earlier.¹²

The reconstituted Mb solutions were concentrated to *ca.* 4–10 mmol dm^{-3} using Amicon Centricon-10 concentrator tubes. FTIR and VCD measurements were obtained by using a *ca.* 27 μm pathlength calcium fluoride cell and a Nicolet 800 FTIR instrument equipped with a VCD accessory constructed at the University of Pittsburgh. IR absorption values were typically 0.03 absorption units. Typical VCD measurements showed ΔA values of 5×10^{-5} absorption units after *ca.* 18 000 scans. Anisotropy ratios were calculated from the ratios of the VCD and IR integrated peak areas.

Results and Discussion

Fig. 1 shows the molecular structure of iron porphyrins where the substituent positions are numbered, while Table 1 relates the peripheral substitution pattern to the haem type. Fig. 2 illustrates the near-haem globin structure for horse Mb azide as deduced from X-ray diffraction measurements.¹⁷ The haem resides in a pocket in the protein; the peripheral vinyl groups dock deep in the pocket while the propionic acid substituents extend towards the aqueous pocket opening.⁷ The haem iron is covalently attached to the proximal histidine. The sixth ligand, azide, is tilted by 69° from the normal and is in close contact with the distal histidine which appears to hydrogen bond to it.¹⁷ The azide penultimate nitrogen is in close contact with the E-11 Val amino acid which presumably constrains the ligand-binding geometry.

Fig. 3(a) shows a typical VCD and IR spectrum for reconstituted horse MbN₃. The absorption peaks at 2022 and 2044 cm^{-1} result from the antisymmetric stretch of azide bound to low-spin and high-spin irons, respectively;⁹ the iron exists in a thermal spin state equilibrium for azide complexes. A single, anomalously large and negative VCD peak is found for only the low-spin azide complex at *ca.* 2023 cm^{-1} . The VCD spectrum

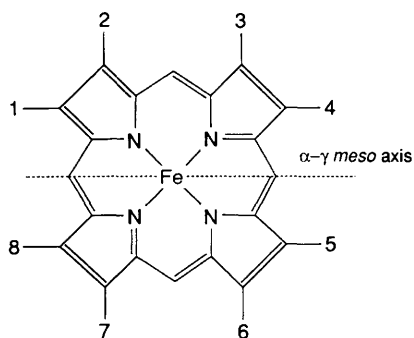


Fig. 1 Molecular structure of iron porphyrins where the substituent groups are numbered. Table 1 relates the substituent pattern to the porphyrin type.

Table 1 Position of substituent groups for protoporphyrin IX, deuterioporphyrin IX, protoporphyrin IX dimethylester and etioporphyrin I

position	proto	deuterio	DME	ETP
1	M	M	M	M
2	V	H	V	E
3	M	M	M	M
4	V	H	V	E
5	M	M	M	M
6	P	P	Es	E
7	P	P	Es	M
8	M	M	M	E

Side-chain abbreviations: M, $-\text{CH}_3$; V, $-\text{CH}_2=\text{CH}_2$; H, $-\text{H}$; P, $-\text{CH}_2\text{CH}_2\text{COOH}$; E, $-\text{CH}_2\text{CH}_3$; Es, $-\text{CH}_2\text{CH}_2\text{COOCH}_3$.

of Mb reconstituted with the natural haem is identical to that of the original native Mb. We have not altered the protein structure during the reconstitution in any way we can detect with VCD, IR absorption or UV visible absorption spectral measurements. τ

Dependence on Haem Peripheral Substitution

We investigated the role of the peripheral vinyl and propionic acid groups on the VCD signal by incorporating iron(III) porphyrins with different peripheral substitution pat-

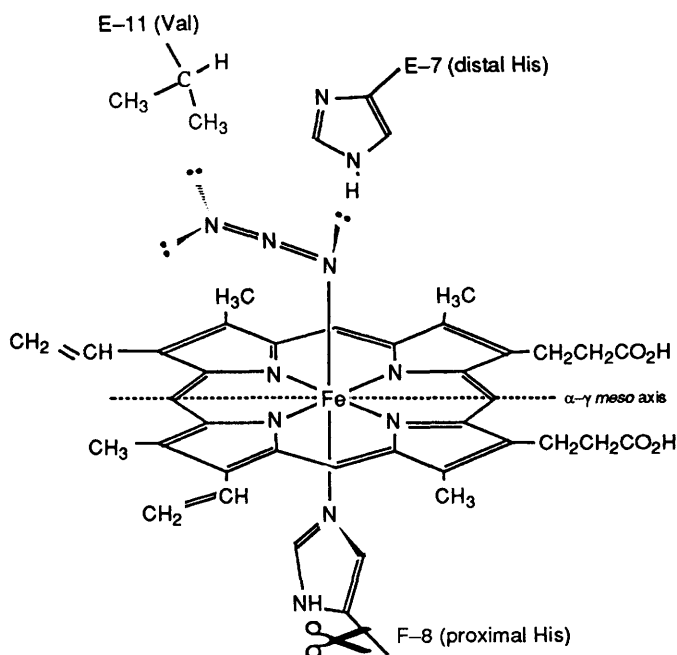


Fig. 2 Haem structure and proximal and distal environment showing the haem and bound azide ligand interactions with the E-11 Val and E-7 His in the distal haem pocket and the relative orientation of the proximal F-8 His. The H93g mutant Mb has no bond between the proximal histidine and the polypeptide chain.

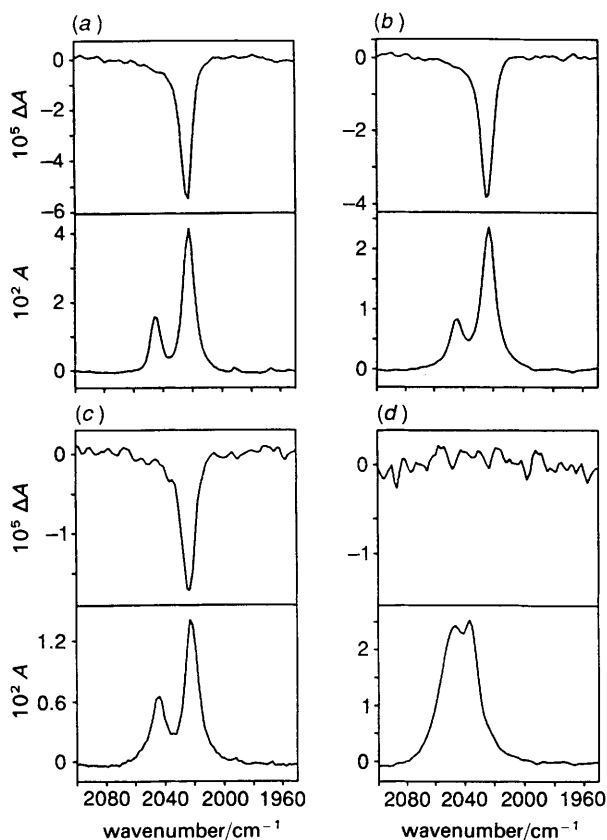


Fig. 3 IR absorption (4 cm^{-1} resolution) and VCD (4 cm^{-1} resolution) spectra of: (a) iron(III) protoporphyrin IX haem reconstituted horse MbN₃; (b) iron(III) protoporphyrin IX dimethylester haem reconstituted horse MbN₃; (c) iron(III) etioporphyrin I haem reconstituted horse MbN₃; (d) Mn³⁺ protoporphyrin IX haem reconstituted horse MbN₃. Protein samples were *ca.* 5–10 mmol dm⁻³ in azide-bound haem and were buffered at *ca.* pH 7 with 0.1 mol dm⁻³ phosphate buffer. All spectra were measured in a 26 μm CaF₂ cell.

terns. These studies examined whether the vinyl groups determine the VCD intensity by giving rise to a sense for the magnetic dipole transition charge circulation,^{3a} or whether peripheral substituents affect the VCD owing to alterations in the haem orientation within the globin pocket.

We repeated our previous measurement⁹ of deuterohaem reconstituted Mb, where the vinyl groups are replaced by hydrogen atoms (Table 2). Once again, we find essentially no change in the VCD anisotropy or in the IR absorption spectrum due to vinyl group substitutions; obviously the vinyl groups are unimportant for determining the VCD anisotropy. In addition, we expect modest alterations in the binding of this non-natural haem in the cavity since any preferences for orientation induced by the vinyls is removed and the haem may show small alterations in its binding geometry. Large changes are excluded since the binding for the haem ring is very well defined even for major substitutions of the haem periphery as well as for removal of the central metal.^{18,19}

We examined the effect of alterations in docking of the haem in the pocket by esterifying the propionic groups that orient towards the exterior of the haem cavity [Fig. 3(b)]. This should result in small changes in the position of the haem in the cavity due to

Table 2 Anisotropy ratios of various haem protein complexes

	$10^4 g$	
	N_3^-	CN^-
<i>native myoglobins</i>		
native horse	-9.5	24
native sperm whale	-9.5	
Asian elephant (E-7 Gln)	-6.4	
<i>myoglobin mutants</i>		
mutant sperm whale (E-7 Gly)	~0.0	
mutant human (E-11 Asn)	~0.0	
mutant sperm whale (F-8 Gly)	+8.4	24
<i>reconstituted myoglobins</i>		
deuteriohaem-substituted	-9.5	
dimethylester-substituted	-9.5	
etioporphyrin I-substituted	-9.5	
Mn protoporphyrin IX-substituted	0.0	
<i>haemoglobins</i>		
human	-8.0	
carp	-8.0	
CTT III	-8.0	

the loss of the propionate salt bridges to the protein.²⁰⁻²² This is likely to result in only small changes in the fit of the haem in the pocket since even large alterations in the propionate substitution pattern results in only modest orientational changes.²⁰⁻²² The fact that we observe no change in the g -value (Table 2) for both removal of the vinyl and esterification of the propionates indicates that the VCD is not sensitive to small alterations of the haem position within the cavity.

A more dramatic haem substitution involves the exchange of all of the peripheral substituents with ethyl and methyl groups in FeETP [Fig. 3(c)]. While this large change removes both the steric interactions with the vinyls and the salt bridges of the propionates, NMR measurements have shown that the FeETP reconstituted Mb adopts a well defined insertion geometry.^{16b} Only hydrophobic packing forces and ligation of the iron to the proximal histidine locate the porphyrin ring in the haem cavity. The observed g -value of the azide complex of FeETP reconstituted horse Mb is identical to that of the native protein (Table 2), which indicates that the VCD intensity is not governed by modest porphyrin relocations within the haem pocket.

This result appears to conflict with the VCD study of the related octaethyl porphyrin (OEP) substituted Mb of Teraoka *et al.*,¹¹ who found a vanishingly small VCD for the azide complex of the FeOEP reconstituted protein. We were unable, however, to incorporate FeOEP, which suggests that they possibly studied a protein where the FeOEP was not in the haem pocket.

The azide complex of Mb shows a VCD signal for only the low-spin complex. Our previous studies of azide-haemoglobin complexes from different species showed similar results; the high-spin complexes show only vanishingly small VCD signals. We suggested⁹ that the large VCD anisotropy required a charge flow conduit from the ligand to the haem, which could only occur for the covalently ligated low-spin azide; the high-spin azide binds ionically. The selectivity of a strong VCD for the low-spin complex and a lack of signal for the high-spin complex was emphasized in our study of carp Hb where the spin-state equilibrium was dramatically altered by adding allosteric effectors. In this case the protein structural change induces a large increase in the high-spin concentration. Although the resulting protein structural change dramatically affects the

spin-state energy difference, it causes no change in the VCD g -value of the low-spin complex, and the high-spin complex still shows no VCD signal.

Dependence upon Metal and Spin State

Mn^{3+} is capable of exchanging for the iron of haem, and this metalloporphyrin can be incorporated into apoMb to form a high-spin complex which binds azide.^{14,23,24} We reconstituted the protein with Mn^{3+} haem and found that no measurable VCD signal occurs from either of the two high-spin azide complexes of Mn^{3+}Mb [Fig. 3(d) and Table 2]. Mn^{3+} is thought to bind azide in two different positions relative to the haem plane; in one orientation the Mn occurs below the plane of the haem and away from the azide ligand, while in the other orientation it occurs above the haem plane, closer to the azide ligand.¹⁴ In this case the azide–Mn bond is shorter and stronger. These two species, as well as free azide, give rise to the IR absorption doublet shown in Fig. 3(d).

Dependence upon Ligand Identity

Fig. 4(b) shows that CN^- ligated to the haem iron also shows a strong VCD intensity as earlier suggested by Teroaka *et al.*¹¹ The CN^- complex is completely low spin. The anisotropy is somewhat larger than that for the azide complex, but the sign is opposite to that of azide ($g = +2.4 \times 10^{-3}$). The signal-to-noise ratio is less than that for azide because of the decreased CN^- absorptivity. CN^- binds almost perpendicular to the haem (it is less than 20° off the haem normal in horse,²⁵ sperm whale²⁶ and CTT Hb²⁷), in contrast to azide which binds¹⁷ at *ca.* 69° . We attempted to measure the VCD signal for the low-spin carbon monoxide complex of iron(II) Mb, but were unable to detect it within our signal-to-noise ratio. We conclude that the g -value must be less than 10^{-4} .

Dependence upon Protein Structure

Our previous study⁹ demonstrated that the VCD of azide depends upon the protein structure surrounding the haem. For example, human Hb showed a *ca.* 15% smaller g -value compared with Mb even though their near-haem residues are similar (Table 2). We, however, observe that the g -values for horse and sperm whale Mb are identical, as are the g -values for human and CTT insect Hb (within 5%). Although, we expected similar VCD spectra for the closely related sperm whale and horse Mb (because the near-haem residues are almost identical), the essentially identical VCD g -values for the different human and insect Hb was surprising. The lack of sensitivity of the g -value to what we thought to be significant differences in near-haem protein structure was consistent with the identical g -values of carp Hb in the presence and absence of allosteric effectors. These allosteric effectors switch the protein from its *R* to its *T*-state conformation. Although the protein quaternary conformation dramatically alters the spin-state equilibrium, the low-spin azide g -value is unaltered. Similarly, no observable VCD alteration occurred for human Hb upon switching its conformation from the *R* to the *T* state by allosteric effectors.

Distal Amino Acid Substitutions

We, however, do find⁹ that substitutions of amino acids on the distal side dramatically alter the VCD (Table 2). The replacement of the E-7 distal His by glycine in a mutant sperm whale Mb (H64G) causes the VCD signal of the azide complex to disappear. Replacement of the distal His by Gln in elephant Mb causes the g -value to decrease by one third (Table 2). Replacement of the E-11 Val by asparagine in human mutant Mb (V68D) causes the VCD to disappear completely. Our previous conclusions were that

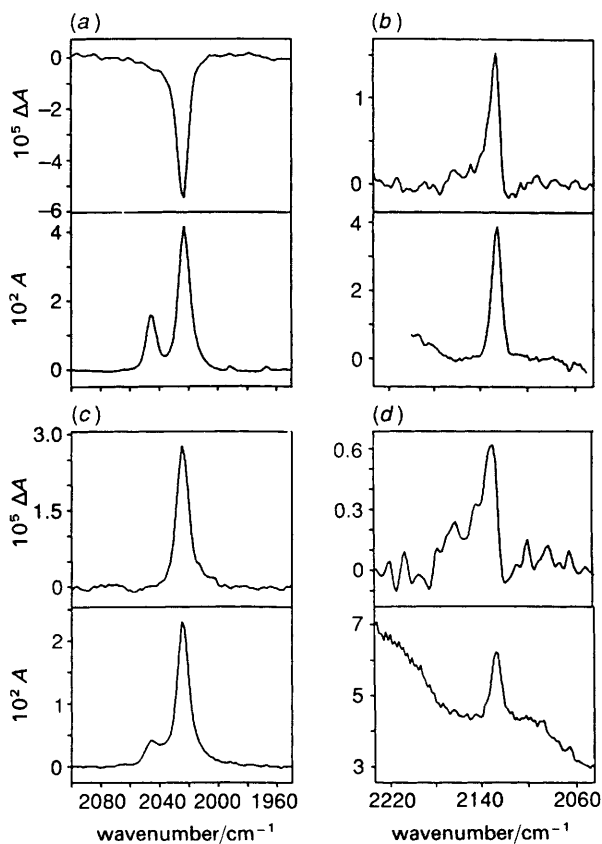


Fig. 4 IR absorption (4 cm^{-1} resolution) spectra and VCD (4 cm^{-1} resolution) spectra of: (a) reconstituted horse MbN₃; (b) reconstituted horse MbCN; (c) H93G sperm whale mutant MbN₃ with imidazole as surrogate F-8 ligand; (d) H93G sperm whale mutant MbCN with imidazole as surrogate F-8 ligand. The protein samples were *ca.* 10 mmol dm^{-3} in azide-bound haem for reconstituted-horse Mb and *ca.* 6 mmol dm^{-3} for H93G mutant sperm whale Mb and were buffered at *ca.* pH 7 with 0.1 mol dm^{-3} phosphate buffer. All spectra were measured in a $26\text{ }\mu\text{m}$ CaF₂ cell.

the E-7 distal His replacement altered the ligand binding geometry, while the E-11 Val mutant (V68D) either changed the geometry or altered the preference of electron flow from the non-bonding penultimate azide orbitals during the azide antisymmetric stretching vibration. We also concluded at that time that the azide VCD signal was most influenced by the distal haem side alterations. This conclusion is derived from the insensitivity of the VCD g -value to the large protein alterations of the CTT Hb compared to the other proteins and the lack of response of the g -values in carp Hb in response to the large spin-state change induced by the allosteric effectors. This spin-state change is thought to correlate with an increased tension at the iron due to strain at the proximal His-Fe linkage.

Proximal Amino Acid Substitutions

We have now examined a mutant sperm whale Mb where the F-8 proximal His is replaced by glycine (H93G).²⁸⁻³⁰ Free imidazole can fill the cleft left by the removed

proximal His and ligate to the haem iron on the proximal side. X-Ray diffraction and NMR measurements indicate a protein structure very close to that of the wild type, and that the major difference is a reorientation of the imidazole haem ring relative to that of the native proximal His ring.^{28–30} The major conceptual conclusion is that this H93G mutant is identical to that of the wild-type protein with the exception that this imidazole ring is no longer covalently linked to the peptide chain (Fig. 2 displays the conceptual alteration as a cutting of the bond between the proximal histidine imidazole ring and the protein). The imidazole ring has been freed from some of the constraints that prevent it from finding its minimum-energy ligation geometry to the Mb bound haem.

Fig. 4(c) shows that the IR absorption spectrum of this H93G Mb mutant azide complex is very similar to that of the wild type, and shows both a weak high-spin azide antisymmetric stretch at higher frequency and a much larger low-spin stretch at lower frequency. The frequencies are within 1 cm^{-1} of that of the wild-type horse Mb. The UV-Vis haem absorption spectrum is also very similar except that the decreased high-spin concentration results in a decreased absorption for the *ca.* 630 nm high-spin charge-transfer absorption band (not shown) and a decreased IR absorbance of the high-spin azide band [Fig. 4(c)]. The VCD dramatically changes; the sign of the azide VCD reverses, while the magnitude decreases by *ca.* 15%. We have also examined the 2-methyl imidazole (2-MeIm) complex of this protein. We expect that the 2-MeIm ligand will be forced to bind with an elongated N-Fe bond owing to the steric constraint imposed by the 2-methyl substituent. In agreement, the absorption spectrum of the 2-MeIm liganded complex is similar to that of the imidazole complex, except that the concentration of the high-spin species appears to increase since the absorbance of the 630 nm absorption band increases (not shown). As expected, the high-spin IR azide stretching band absorbance also increases. The *g*-values of both imidazole complexes are identical. This behaviour is similar to that observed for the carp Hb azide, where the change in spin state was not accompanied by any observable change in the VCD anisotropy. Apparently, the VCD is not sensitive to strain at the proximal histidine-iron bond.

Previous studies of the structure of the cyanide and the aquo complexes of the H93G mutant^{28–30} indicate that a significant rotation occurs for the imidazole ring about the bond connecting the iron to the imidazole nitrogen; in the wild type the ring comes close to lying along the N-Fe-N axis, while in the mutant it is closer to 45° . Only a small reorientation occurs for the imidazole ring plane with respect to the haem plane between the native protein and the mutant; the angle between the normals to the planes of the imidazole ring increases from 87.5° in the wild type to 75° in the H93G mutant.

In contrast to the results for azide complex, the CN^- complex shows a very similar *g*-value with identical sign for the wild type and the H93G mutant. There are two possibilities to explain this inconsistent result. If the VCD sign is controlled by the relative orientation of the ligand axis relative to that of the imidazole plane, the change in the imidazole-ring rotation in the azide complex of the mutant compared to the wild type would dramatically affect the VCD sign. In contrast, little change would occur for CN^- which binds almost end on. The less likely possibility is that a much more dramatic structural alteration occurs between the native protein and the mutant for the azide complex compared with the CN^- and aquo mutant complexes. The X-ray structure of the mutant azide complex should become available in the near future.

The IR absorption bandshapes and maxima of most of the low-spin azide complexes and the cyanide complexes differ somewhat from those of the VCD. For the azide complexes the VCD maxima shift upwards by *ca.* 1 cm^{-1} . The cyanide complex shows the largest difference with a *ca.* 2 cm^{-1} shift of the VCD maximum and a large shift in the bandshape. These differences are presumably the result of a distribution of ligand geometries in the protein which have very different anisotropies. The only protein where the bandshape and maxima are identical within the signal-to-noise ratios is the azide complex of the H93G mutant. Possibly, the loss of constraints on the haem geometry

results in a single-liganded species. However, this possibility is made tenuous by the fact that the largest difference occurs for the H93G cyanide mutant. The band-shape differences indicate that the VCD band shape is inhomogeneously broadened by liganded protein substates and that the VCD is more affected by this than is the IR absorption. The azide VCD band shape is always asymmetric and the cyanide complex shows a high-frequency shoulder in both the IR absorption and in the VCD spectra.

VCD Mechanism

Our earlier work suggested that the anomalously large VCD g -values for the haem proteins resulted from a very large magnetic moment, m , associated with a ring current in the haem. This will result in a very large g -value because:

$$g = 4 \text{IM}(\boldsymbol{\mu} \cdot \mathbf{m})/|\boldsymbol{\mu}|^2$$

The dipole transition moment, $\boldsymbol{\mu}$, for the ligand stretching vibration should be aligned dominantly along the ligand axis which has a large component along the normal to the haem plane. If the ratio of m to $\boldsymbol{\mu}$ were constant for azide and cyanide, we would expect that the cyanide would have a *ca.* three-fold larger g -value than azide, since the cyanide ligand is perpendicular to the haem rather than inclined by *ca.* 69° . This is very close to the relative magnitudes. Obviously, the situation is much more complex; the change in sign of the azide g -value for the H93G mutant indicates the intimate involvement of the proximal histidine ring in the mechanism. Possibly the orientation of the magnetic moment is determined by the orientation of the proximal histidine relative to the haem pyrrole nitrogens and the ligand. The source of the magnetic moment cannot be localized in the plane of the proximal histidine ring since the CN^- ligand transition moment would then be almost normal to the magnetic moment.

The mechanism for VCD can also be cast in terms of the vibrational mixing of electronic transitions into the vibrational transition, where the lowest-energy transitions would be most heavily weighted owing to the energy denominator of the perturbation expression.⁵ We attempted to monitor the lowest-energy haem transitions in order to correlate their anisotropy relative to that of the ligand stretching vibration. As discussed previously,⁹ removal of the distal histidine in the H64G mutant causes the VCD anisotropy of the azide antisymmetric stretch to vanish. Fig. 5(a), which shows the absorption and electronic CD spectra of native sperm whale MbN₃, and this H64G mutant, shows that the anisotropy of the low-spin electronic CD band at 586 nm decreases by 50%. The high-spin, *ca.* 630 nm charge-transfer band absorption increases, indicating an increased high-spin concentration. However, the g -value of this CD band decreases. We see a clear correlation in this case between the magnitude of the anisotropy of the lowest-lying electronic transitions and the VCD spectrum for the azide complex. The *ca.* 600 nm absorption bands are thought to have some charge-transfer character due to the involvement of ligand and metal orbitals in the electronic excited state.

In contrast, the azide complexes of native horse Mb and the imidazole and 2-MeIm complexes of the H93G mutant [Fig. 5(b)] show very similar CD spectra where the main difference is a larger trough at *ca.* 560 nm. This small change accompanies the strikingly dramatic sign reversal of the VCD of the azide mutant. Possibly the electronic CD only correlates with the magnitude of the VCD and is independent of the sign.

There are lower-lying charge transfer absorption bands at *ca.* 6000 cm^{-1} for azide and CN^- complexes which could also couple to the vibration.³¹ These absorptions are relatively weak and are reported to show no CD spectrum. They show a complex vibronic envelope which does not obviously have a *ca.* 2000 cm^{-1} periodicity. Future studies will be required to determine if these electronic transitions are important in the VCD mechanism.

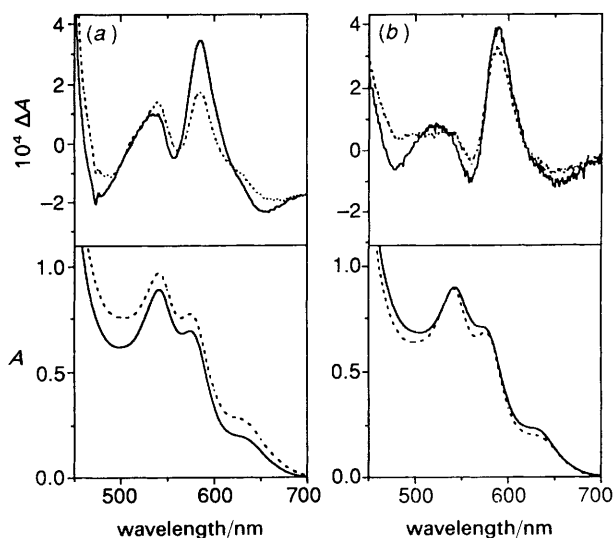


Fig. 5 Electronic absorption and electronic CD of (a) sperm whale MbN₃ (—) and the H64G sperm whale Mb mutant (.....) where the E-7 distal His is replaced by a glycine and (b) horse MbN₃ (—) and the H93G sperm whale Mb mutant (.....) where the F-8 proximal His is replaced by glycine. For this protein a 2-methyl imidazole ligand binds in the cleft left by the proximal His and binds to the haem iron. Similar spectra occur when imidazole replaces the 2-methyl imidazole. The main difference observed is a decrease in absorption of the *ca.* 630 nm high-spin absorption band. The protein haem concentration was 80 μM in 1.0 mol dm⁻³ phosphate buffer, pH 7.0.

A significant VCD *g*-value for an azide antisymmetric ligand stretching vibration does not require a haem ring. Fig. 6 shows the VCD of the antisymmetric ligand stretching vibration of azide bound to haemerythrin which is a non-haem metalloenzyme. The *g*-value is calculated from the spectrum to be -7.4×10^{-5} which is *ca.* 10-fold smaller

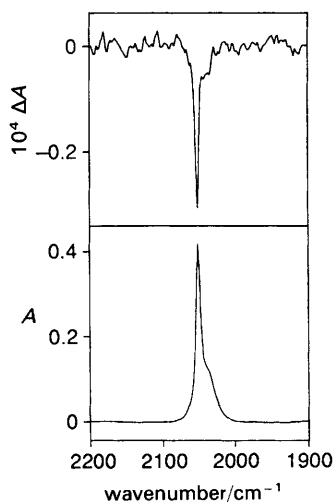


Fig. 6 Absorption spectrum and VCD spectrum of azidomethemerythrin. The protein is *ca.* 25 mmol dm⁻³ in 50 mmol dm⁻³ TRIS-acetate buffer at pH 8.0 with a small excess of azide. The IR absorption spectrum shows two bands, the iron-bound azide band and a weaker band from the excess azide present in solution.

than that of the haem proteins. Although the g -value is smaller than for haem-bound azide, it is still very large for a vibration localized on a non-chiral molecular fragment whose chirality is induced by an attached chiral site. Azide is coordinated in a bent end-on fashion to one of the high-spin Fe^{3+} of the diiron site of haemerythrin.³²

Conclusions

We demonstrate that VCD can be used to examine ligand binding in haem and non-haem metalloenzymes. The Hb and Mb anisotropies depend upon the protein structure both on the distal side and upon the binding of the proximal histidine and the iron. The difference in the ligand-stretching band shape between the IR and VCD indicates that the VCD is more sensitive to protein ligation substates than is the IR absorption spectrum. We demonstrate the potential sensitivity of the ligand VCD spectra for probing ligand binding in metalloenzymes. The spectra depend upon steric and hydrogen-bonding interactions of the ligand with surrounding amino acid residues and the details of the attachment of other ligands to the metal. Unfortunately, there is still insufficient information to develop a model for the VCD mechanisms which can be used to obtain protein structural insights.

We gratefully acknowledge helpful conversations with Professor Larry Nafie at Syracuse University and thank him for his help in initiating these studies. We thank Peter Larkin for helping in CD measurements of the H64G mutant. We thank NIH grants 1R01-GM30741-13 (to S.A.A.) and GM403:8 (to D.M.K.) for financial support.

References

- 1 L. D. Barron, *Molecular Light Scattering and Optical Activity*, Cambridge University Press, Cambridge, 1982.
- 2 T. A. Keiderling, in *Practical FTIR Spectroscopy*, ed. J. R. Ferraro and K. Krishnan, Academic Press, San Francisco, 1990, p. 203.
- 3 (a) T. B. Freedman and L. A. Nafie, in *Topics in Stereochemistry*, ed. E. Eliel and S. H. Wilen, Wiley, New York, 1987, vol. 17, p. 113; (b) T. B. Freedman and L. A. Nafie, in *Modern Nonlinear Optics, Part 3*, ed. M. Evans and S. Kielich, Adv. Chem. Phys. Ser. 1994, vol. 85, p. 207.
- 4 (a) P. L. Polavarapu, in *Fourier Transform Infrared Spectroscopy*, 1985, 4, 61; (b) P. L. Polavarapu, in *Vibrational Spectra and Structure*, ed. J. R. Durig, Elsevier, Amsterdam, 1984, vol. 13, p. 103.
- 5 (a) P. J. Stephens and M. A. Lowe, *Annu. Rev. Phys. Chem.*, 1985, 36, 213; (b) A. E. Hansen, P. J. Stephens and T. D. Bourman, *J. Phys. Chem.*, 1991, 95, 4255.
- 6 (a) T. A. Keiderling, *Appl. Spectrosc. Rev.*, 1981, 17, 189; (b) P. Bour and T. A. Keiderling, *J. Am. Chem. Soc.*, 1992, 114, 9100; (c) P. Pancoska, S. C. Yasui and T. A. Keiderling, *Biochemistry*, 1989, 28, 5917.
- 7 R. E. Dickerson and I. Geis, in *Hemoglobin, Structure, Function, Evolution, and Pathology*, Benjamin Cummings, Menlo Park CA, 1983.
- 8 C. Marcott, H. A. Havel, B. Hedlund, J. Overend and A. Moscowitz, in *Optical Activity and Chiral Discrimination*, ed. S. F. Mason, D. Reidel, New York, 1979, p. 289.
- 9 R. W. Bormett, S. A. Asher, P. J. Larkin, W. G. Gustafson, N. Ragunathan, T. B. Freedman, L. A. Nafie, S. Balasubramanian, S. G. Boxer, N-T. Yu, K. Gersonde, R. W. Noble, B. A. Springer and S. G. Sligar, *J. Am. Chem. Soc.*, 1992, 114, 6864.
- 10 S. A. Asher, R. W. Bormett, P. J. Larkin, W. G. Gustafson, N. Ragunathan, T. B. Freedman, L. A. Nafie, N-T. Yu, S. Gersonde, K. Noble, B. A. Springer, S. G. Sligar, R. W. Balasubramanian and S. G. Boxer, *Spec. Publ. R. Soc. Chem.*, 1991, 94, 139.
- 11 J. Teraoka, K. Nakamura, Y. Nakahara, Y. Kyogoku and J. Sageta, *J. Am. Chem. Soc.*, 1992, 114, 9211.
- 12 (a) I. M. Klotz and D. M. Kurtz Jr., *Acc. Chem. Res.*, 1984, 17, 16; (b) P. C. Wilkins and R. G. Wilkins, *Coord. Chem. Rev.*, 1987, 79, 195; (c) F. Bonomi, R. C. Long and D. M. Kurtz Jr., *Biochim. Biophys. Acta*, 1989, 999, 147.
- 13 F. W. Teale, *Biochim. Biophys. Acta*, 1959, 35, 543.
- 14 B. Hoffman and Q. Gibson, *Biochemistry*, 1976, 15, 3405.
- 15 M. Tamura, T. Asakura and T. Yonetani, *Biochim. Biophys. Acta*, 1973, 295, 467.
- 16 (a) S. Neya, N. K. Funasaki and K. Imai, *J. Biol. Chem.*, 1988, 263, 8810; (b) *Biochim. Biophys. Acta*, 1989, 996, 226.

- 17 L. Stryer, L. C. Kendrew and H. C. Watson, *J. Mol. Biol.*, 1964, **8**, 96.
- 18 K. Miki, Y. Y. II, M. Yukawa, A. Owatari, Y. Hato, S. Harada, Y. Kai, N. Kasai, Y. Hata, N. Tanaka, M. Kakudo, Y. Katsube, K. Kawabe, Z. Yoshida and H. Ogoshi, *J. Biochem.*, 1986, **100**, 269.
- 19 J. T. L. Lecomte and M. J. Cocco, *Biochemistry*, 1990, **29**, 11057.
- 20 J. B. Hauksson, G. N. La Mar, R. K. Pandey, I. N. Rezzano and K. M. Smith, *J. Am. Chem. Soc.*, 1990, **112**, 8315.
- 21 G. N. La Mar, S. D. Emerson, J. T. J. Lecomte, U. Pande, K. M. Smith, G. W. Craig and L. A. Kehres, *J. Am. Chem. Soc.*, 1986, **108**, 5568.
- 22 J. B. Hauksson, G. N. La Mar, R. K. Pandey, I. N. Rezzano and K. M. Smith, *J. Am. Chem. Soc.*, 1990, **112**, 6198.
- 23 N-T. Yu and M. Tsubaki, *Biochemistry*, 1980, **19**, 4647.
- 24 M. Tsubaki, R. B. Srivastava and N-T. Yu, *Biochemistry*, 1981, **20**, 946.
- 25 J. F. Deatherage, J. F. Loers, C. M. Anderson and K. Moffat, *J. Mol. Biol.*, 1976, **104**, 687.
- 26 S. D. Emerson and G. N. La Mar, *Biochemistry*, 1990, **29**, 1556.
- 27 W. Steigemann and E. Weber, *J. Mol. Biol.*, 1979, **127**, 309.
- 28 D. Barrick, *Biochemistry*, 1994, **33**, 6546.
- 29 G. D. DePillis, S. M. Decatur, D. Barrick and S. G. Boxer, *J. Am. Chem. Soc.*, 1994, **116**, 6981.
- 30 S. M. Decatur and S. G. Boxer, *Biochemistry*, 1995, **34**, 2122.
- 31 P. J. Stephens, J. C. Sutherland, J. C. Chang and W. A. Eaton, in *Proceedings of the International Conference on Excited States of Biological Molecules*, ed. J. Birks, Wiley Interscience, New York, 1976, p. 434.
- 32 M. A. Holms and R. E. Stenkamp, *J. Mol. Biol.*, 1991, **220**, 723.